

Article

Flotation Separation of Chalcopyrite and Talc Using Calcium Ions and Calcium Lignosulfonate as a Combined Depressant

Qiongyin Mai ^{1,2,†}, Hanyu Zhou ^{1,2,†} and Leming Ou ^{1,2,*}

¹ School of Minerals Processing and Bioengineering, Central South University, Changsha 410083, China; maiqiongyin@csu.edu.cn (Q.M.); 205611038@csu.edu.cn (H.Z.)

² Key Laboratory of Hunan Province for Clean and Efficient Utilization of Strategic Calcium-Containing Mineral Resources, Central South University, Changsha 410083, China

* Correspondence: olmpaper@csu.edu.cn; Tel.: +86-0731-8883-0913

† Q.M. and H.Z. contributed equally to this work.

Abstract: As a major gangue mineral in sulfide ores, talc is difficult to separate from chalcopyrite in the flotation process due to its natural floatability, which affects the subsequent smelting process. In this study, the effects of calcium ions and calcium lignosulfonate (CLS) as a combination depressant for talc were systematically investigated along with the fundamental mechanisms. The results of our flotation tests showed the talc floating can be effectively depressed via the combination depressant effect of calcium ions and CLS over the pH range of 6–12. Measurements of the adsorption capacity, zeta potential, and Fourier transform infrared (FTIR) showed an enhancement of the adsorption capacity and adsorption strength of CLS on the talc surface after calcium ions were added. This result indicates that calcium ions adsorbed onto the talc, neutralized the negative charge on the surface of talc, generated the binding site with CLS, and formed the [talc-Ca²⁺/Ca(OH)⁺-CLS] system by strong adsorption. Further, the coverage rate of CLS on talc was significantly improved after the addition of calcium ions, as shown in the AFM imaging.

Keywords: chalcopyrite; talc; calcium lignosulfonate; calcium ion; adsorption



Citation: Mai, Q.; Zhou, H.; Ou, L. Flotation Separation of Chalcopyrite and Talc Using Calcium Ions and Calcium Lignosulfonate as a Combined Depressant. *Metals* **2021**, *11*, 651. <https://doi.org/10.3390/met11040651>

Academic Editor: Jean-François Blais

Received: 19 March 2021

Accepted: 13 April 2021

Published: 16 April 2021

Publisher's Note: MDPI stays neutral with regard to jurisdictional claims in published maps and institutional affiliations.



Copyright: © 2021 by the authors. Licensee MDPI, Basel, Switzerland. This article is an open access article distributed under the terms and conditions of the Creative Commons Attribution (CC BY) license (<https://creativecommons.org/licenses/by/4.0/>).

1. Introduction

The use of copper, a key metal in the green energy transition, is expected to rise as long as the demand for electric cars, solar, and wind power continues to rise [1]. At present, copper is generally obtained by flotation of copper sulfide [2]. Talc (Mg₃Si₄O₁₀(OH)₂) is a widely distributed layered silicate mineral with ionic bonds in the layers and molecular bonds between the layers [3–5]. It possesses superb natural floatability due to its non-polar surface and highly hydrophobicity [6]. In the process of crushing and grinding, talc easily produces a slime phenomenon and adheres to the surface of the target mineral, which greatly affects the flotation separation, resulting in an increase in the MgO content in the concentrate and affecting the subsequent smelting process [7–11]. Copper sulfide minerals are often associated with magnesium-bearing silicate gangue minerals such as talc and serpentine, while flotation is a commonly used method for separating copper sulfide minerals and talc [12]. Three main strategies are currently employed by the mining industry to separate chalcopyrite from talc: (1) Reverse flotation. Preferential flotation of talc using collectors, with metal loss as a main drawback [13]. (2) Acid leaching. The avoidance of using depressants to depress talc flotation. Instead, talc is removed by acid leaching after naturally entering the concentrate. A disadvantage of this method is that the talc continues to circulate in the process, which increases the complexity of the production process [14]. (3) Depression of talc with high-efficiency depressants. However, the existing beneficiation technology has been unable to meet the needs of efficient development and utilization of lean ore [15]. Hence, the study of an efficient talc depressant is the key to realize the flotation separation of copper sulfide minerals and talc. Several commonly used

talc depressants include guar gum, xanthan gum, starch, and carboxymethyl cellulose (CMC) [16–18]. Shi Qing et al. showed that xanthan gum obviously depressed talc flotation, with few effects on chalcopyrite flotation at pH 8. The adsorption of xanthan gum on the talc surface is achieved through physical action, with hydrophobic interactions acting as a main driving force [19]. Parolis et al. studied the effect of divalent cations Ca^{2+} and Mg^{2+} and monovalent K^{+} ions on the behavior of CMC adsorption. They found that Ca^{2+} and Mg^{2+} were far more efficient in promoting the adsorption of CMC onto talc surfaces than K^{+} ions [16]. Note that CMC is an effective talc depressant in copper sulfide flotation. However, CMC can hardly be fully dissolved during production, so the flotation separation of chalcopyrite and talc is still a problem [20]. Therefore, it is of great significance to find a reagent with high selectivity for talc depression in copper sulfide flotation.

Calcium lignosulfonate (CLS) is a high-molecular anionic polyelectrolyte, which is a by-product of cellulose extracted from wood processing [21]. CLS possesses excellent wettability, dispersibility, and adsorption performances due to its functional groups, including sulfonic and carboxyl groups as well as alkyl and aryl groups [22]. In the past decades, lignosulfonate has been used as a pyrite depressant in the flotation of chalcopyrite and is also a quartz depressant in the flotation of smithsonite [23,24]. Run-qing Liu et al. studied the effect of CLS on the separation of chalcopyrite from pyrite. They noticed that CLS covered the surface of pyrite and prevented the formation of dixanthogen on the pyrite surface, which made the pyrite surface hydrophilic and thus separated the pyrite from the chalcopyrite [25].

The purpose of this study is to use CLS as a talc depressant to separate chalcopyrite and talc by flotation. The depression effect of CLS in the presence or absence of calcium ions was studied through flotation tests. The adsorption capacity, zeta potential, and AFM tests were used to analyze the morphology of the polymer adsorption layer on the hydrophilic surface and to study the difference in the adsorption layer on the talc surface with or without calcium ions in CLS. The depression mechanisms were summarized based on the experimental results.

2. Materials and Methods

2.1. Materials

Chalcopyrite and talc were obtained from Hubei and Guangxi, respectively. The mineral samples were finely ground in an XQM-4 planetary ball mill and sieved into several particle sizes with 200 mesh and 400 mesh standard screens dividing them into three grades. Particles with a size of 38–74 μm were used for flotation, adsorption, and FTIR tests (Shimadzu, Kyoto, Japan), while those less than 38 μm were ground with an agate mill to below 5 μm for zeta potential measurements. The chemical composition analysis of chalcopyrite and talc was performed using an X'Pert3 POWder X-ray diffractometer (XRD, PANalytical, Almelo, The Netherlands) and Axios mAX X-ray fluorescence spectrometer (XRF, PANalytical, Almelo, The Netherlands). According to XRD (Figure 1) and elemental analysis (Table 1), the purity of the chalcopyrite and talc used in the test was relatively high and met the test requirements. CLS, potassium butylxanthate (PBX), hydrochloric acid, sodium hydroxide, and anhydrous calcium chloride were all analytical pure agents obtained from Tianjin Chemical Reagent Factory (Tianjin, China), and the experimental water was deionized water. The monomeric molecule structure of CLS is shown in Figure 2.

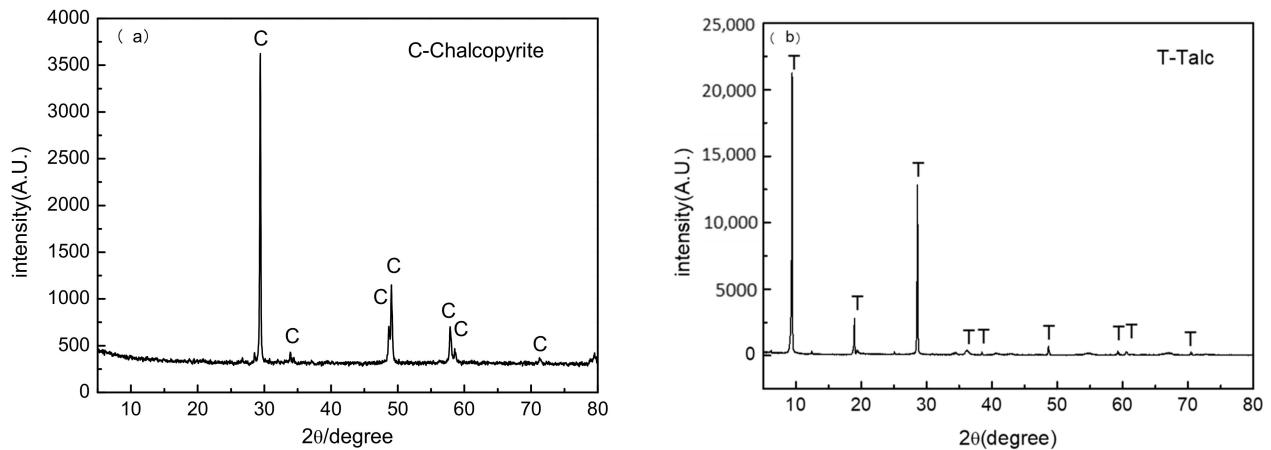


Figure 1. XRD patterns of pure chalcopyrite (a) and talc (b) samples.

Table 1. Chemical composition of chalcopyrite and talc.

Sample	Mass Fraction/%					
	Cu	TFe	S	MgO	SiO ₂	Al ₂ O ₃
Chalcopyrite	33.635	29.764	33.584	-	2.782	-
Talc	-	0.774	-	29.561	64.830	0.366

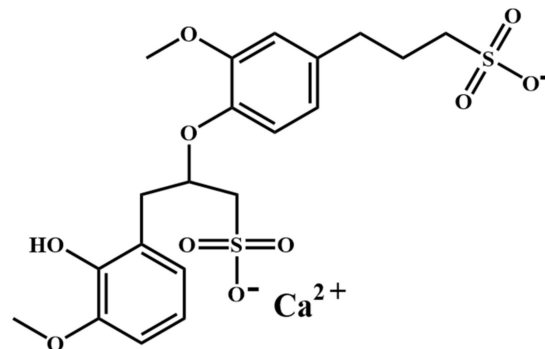


Figure 2. Monomeric molecular structure of CLS.

2.2. Flotation Experiment

Flotation experiments were carried out in an XFG-C flotation machine (Jilin Prospecting Machinery Factory, Changchun, China) with a 40 mL plexiglass cell; 2 g of minerals and 40 mL of deionized water were weighed and stirred in a flotation cell. Then, hydrochloric acid or sodium hydroxide was used to adjust the pH of the pulp, after which a calcium chloride solution, CLS depressant, potassium butylxanthate (PBX) collector, and MIBC frother were successively added to the pulp. The froth obtained by flotation and the product in the cell were filtered, dried, and weighed, and the yield was calculated as the recovery rate, while the flotation separation efficiency of the artificial mixed minerals was calculated by the Douglas formula, as shown in Equation (1).

$$E = \frac{\varepsilon - \gamma}{100 - \gamma} \cdot \frac{\beta - \alpha}{\beta_{\max} - \alpha} \times 100\% \quad (1)$$

α —The primary ore grade, %.

β —The concentrate grade, %.

γ —The concentrate yield, %.

ε —Recovery, %.

β_{\max} —Pure mineral grade, %.

2.3. Adsorption Capacity Experiment

A variatorTOC analyzer was employed for the adsorption capacity experiment (Elementar, Langensfeld, Germany): 2 g mineral (chalcopyrite/talc) and 40 mL deionized water were weighed and then mixed well in a flotation cell. The pH of the pulp was adjusted by hydrochloric acid or sodium hydroxide, and then calcium ions and CLS were added according to the flotation conditions. According to Equation (2), the adsorption density of CLS on the mineral surface can be obtained [25].

$$\Gamma = \frac{(C_o - C_e)V}{mA} \quad (2)$$

Γ —Adsorption density of calcium lignosulfonate on the mineral surface, mg/m².

C_o —Original concentration of CLS, mg/L.

C_e —Supernatant concentration of calcium lignosulfonate, mg/L.

V —Volume of solution, mL.

m —Quality of minerals, g.

A —Specific surface area of minerals, m²/g.

The specific surface areas of chalcopyrite and talc were 2.224 m²/g and 2.626 m²/g, respectively, determined by the BET method.

2.4. Zeta Potential Measurements

The zeta potentials were measured using a Coulter Delsa440sx zeta analyzer machine (Colloidal Dynamics, LLC, Ponte Vedra Beach, FL, USA). The talc samples were ground until the particle size was less than 5 µm; then, 40 mg talc and 40 mL potassium chloride electrolytic solution were added to a beaker. The pulp pH was adjusted, and the agent was added according to the test requirements. After stirring with a magnetic agitator for 10 min, a certain amount of pulp was extracted, and its zeta potential value was measured with the zeta potential analyzer.

2.5. Fourier Transform Infrared Spectrometry (FTIR) Analysis

In order to characterize the interaction between depressants and minerals, an IRAffinity-1 Fourier Transform Infrared Spectrometer was used to measure the infrared spectra in the range of 400–4000 cm^{−1} with a resolution of 2 cm^{−1}, scanned 30 times.

2.6. AFM Imaging

The samples under different reagent conditions were observed with a Multimode V scanning probe microscope produced by the Veeco Instrument Company, USA (Plainview, NY, USA). The AFM used an RTESP monocrystalline silicon cantilever probe with a scanning rate of 1 Hz, close to 600 nm/s, and all measurements were made at room temperature (25 °C) in air. The talc samples with the dissociated surface were placed in the required reagent solution, stirred for 30 min to reach the absorption equilibrium, and then dried under high-purity nitrogen. Three samples were selected for each test condition for measurement and calculation, and a representative image was produced for each condition. Nanoscope analysis 1.80 software was used to calculate the root mean square roughness and peak-to-valley distance (PTV) and to evaluate the surface coverage. According to the thickness difference between the polymer and the smooth stone surface, the polymer apparent layer thickness (Δ PTV) can be obtained [8,26].

3. Results and Discussion

3.1. Flotation Test Results

Figure 3 shows the effect of the amount of collector PBX on the flotation of chalcopyrite and talc. The recovery rate of talc remained high with increased PBX due to its natural floatability, while the recovery rate of chalcopyrite increased with the increase in the reagent concentration. When the dosage of PBX was 50 mg/L, the recovery rate of chalcopyrite

reached the maximum. The results showed that the flotation separation of chalcopyrite and talc could not be achieved without the use of depressants. Figure 4 exhibits the effect of calcium ions on the flotation of chalcopyrite and talc. As shown in Figure 4, the recovery rates of chalcopyrite and talc changed insignificantly with the increase in the calcium ion concentration. Therefore, the flotation recoveries of chalcopyrite and talc were not only affected by the change in the calcium ion concentration.

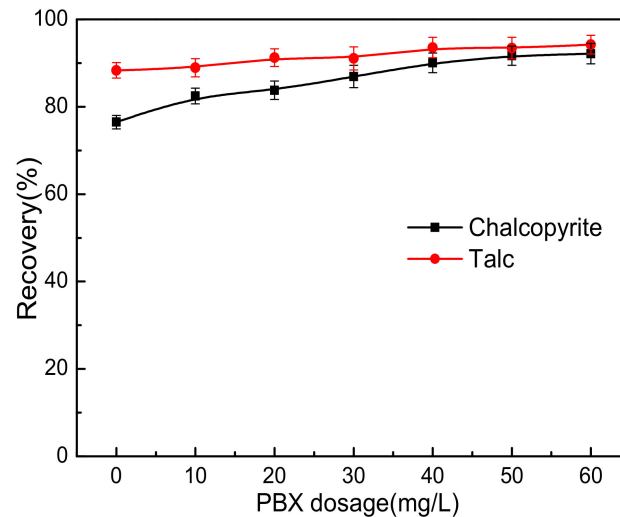


Figure 3. Effect of PBX dosage on the flotation of chalcopyrite and talc ($c(\text{MIBC}) = 0.125 \text{ mL/L}$, $\text{pH} = 8$).

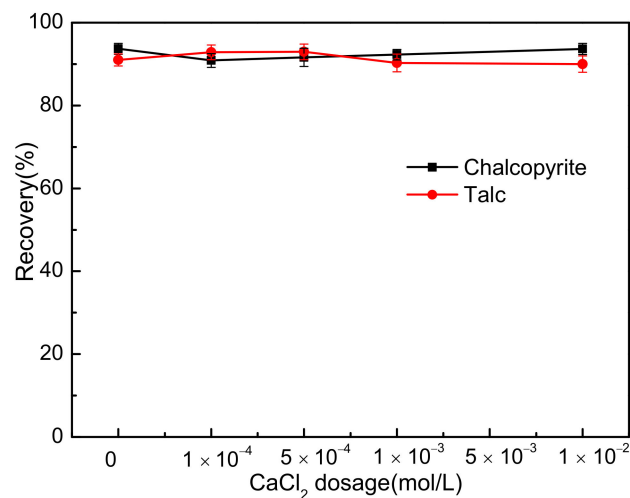


Figure 4. Effect of CaCl_2 dosage on the flotation of chalcopyrite and talc ($c(\text{PBX}) = 50 \text{ mg/L}$, $c(\text{MIBC}) = 0.125 \text{ mL/L}$, $\text{pH} = 8$).

The effects of CLS dosage on chalcopyrite and talc flotation under different calcium ion concentrations are exhibited in Figure 5. As shown in Figure 5a, when the dosage of CLS exceeded 200 mg/L , the depression effect of CLS on chalcopyrite was enhanced by increasing the dosage of the calcium ions. It can be seen from Figure 5b that CLS was an effective depressant of talc. When only the CLS depressant was added to the solution, the talc recovery rate decreased gradually with the increase in the amount of CLS. When the concentration of calcium ions was $1 \times 10^{-3} \text{ mol/L}$, the flotation recovery of talc decreased rapidly with the increase in the dosage of CLS, and the flotation recovery of talc decreased to 6.0% when the dosage of CLS reached 200 mg/L . In Figure 6a, with the increase in pH, the recovery rate of chalcopyrite gradually increased and reached about 88% at $\text{pH} = 6$. When $\text{pH} > 6$, the recovery of chalcopyrite did not change much. As can be seen from

Figure 6b, CLS exhibited a strong depression effect on talc under acidic conditions. With the increase in pH, the depression effect of CLS on talc was weakened when there were no calcium ions or the concentration of calcium ions was low (1×10^{-4} mol/L). When the calcium ion concentration increased, the depression effect of CLS on talc became stronger under a wide pH range. It can be concluded that the flotation separation of chalcopyrite and talc could be achieved in the pH range of 6 to 12 by using CLS as the depressant.

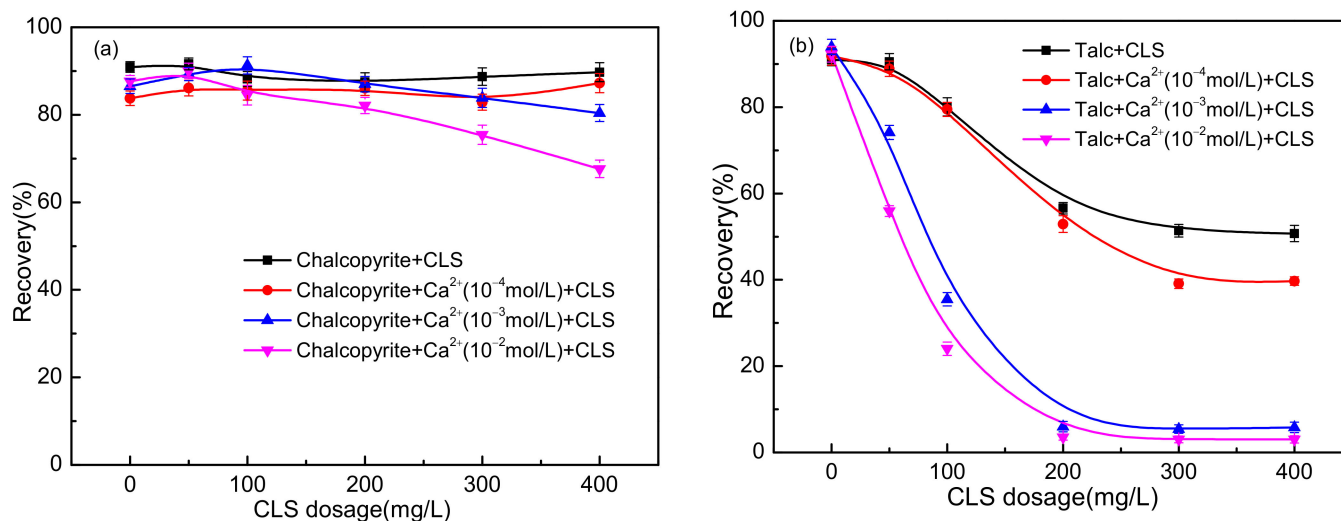


Figure 5. Effects of CLS dosage on the flotation behavior of chalcopyrite (a) and talc (b) in the presence of various Ca^{2+} ions ($c(\text{PBX}) = 50 \text{ mg/L}$, $c(\text{MIBC}) = 0.125 \text{ mL/L}$, $\text{pH} = 8$).

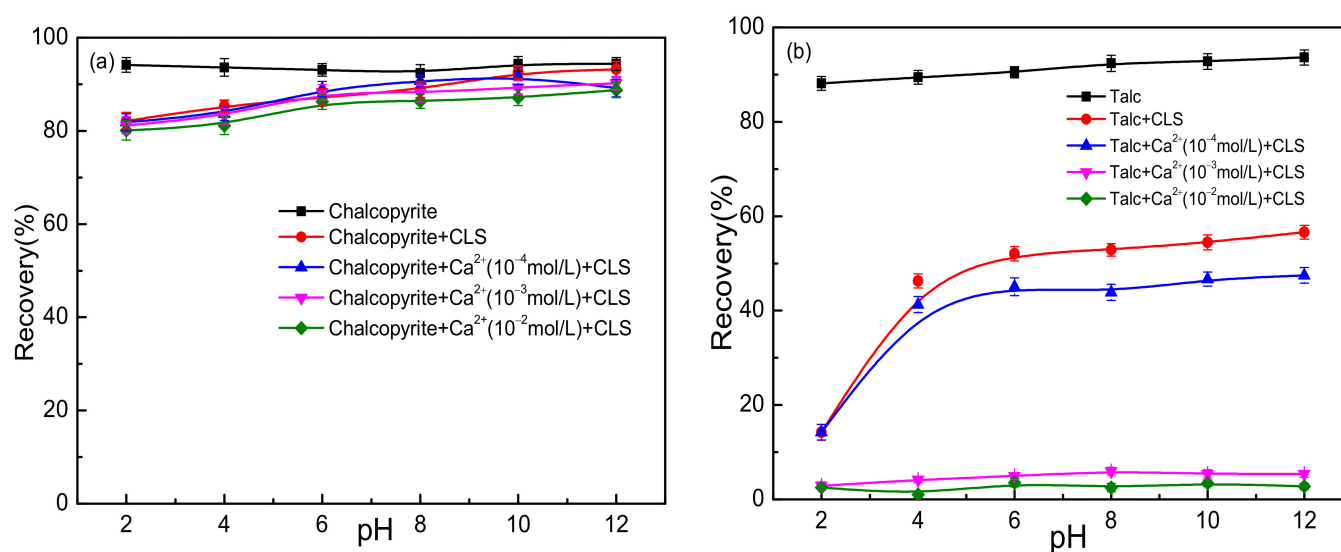


Figure 6. Effect of pH on depression effect of CLS on chalcopyrite (a) and talc (b) in the presence of various Ca^{2+} ions ($c(\text{CLS}) = 200 \text{ mg/L}$, $c(\text{PBX}) = 50 \text{ mg/L}$, $c(\text{MIBC}) = 0.125 \text{ mL/L}$).

Table 2 shows the effects of CLS on the flotation of artificial mixed minerals in the presence or absence of added calcium ions. The results revealed that CLS could effectively realize the separation of chalcopyrite and talc. Compared with the flotation results of single CLS, the combined action of calcium ions and CLS reduced the content of talc in the artificial mixed minerals and improved the recovery of chalcopyrite. The combined action of calcium ions and CLS increased the separation efficiency from 11.7 to 26.3%, which was more beneficial to the flotation recovery of chalcopyrite.

Table 2. Effect of CLS on flotation performance with/without the presence of Ca^{2+} ions ($c(\text{CLS}) = 200 \text{ mg/L}$, $c(\text{Ca}^{2+}) = 1 \times 10^{-3} \text{ mol/L}$, $c(\text{PBX}) = 50 \text{ mg/L}$, $c(\text{MIBC}) = 0.125 \text{ mL/L}$, $\text{pH} = 8$).

Conditions	Product	Yield/%	Grade/%		Recovery/%		Separation Efficiency/%
			Cu	MgO	Cu	MgO	
-	Concentrate	81.5	15.3	17.8	88.7	79.2	2.3
	Tailings	18.5	8.6	20.5	11.3	20.8	
	Feed	100.0	14.0	18.3	100.0	100.0	
CLS	Concentrate	27.9	23.8	6.8	46.2	11.0	11.7
	Tailings	72.1	10.8	21.1	53.8	89.0	
	Feed	100.0	14.4	17.1	100.0	100.0	
Ca^{2+} + CLS	Concentrate	23.4	29.7	3.0	50.0	4.1	26.3
	Tailings	76.6	9.0	21.7	50.0	95.9	
	Feed	100.0	13.9	17.3	100.0	100.0	

3.2. Adsorption Capacity Experimental Results

Figure 7 presents the adsorption behavior of CLS on chalcopyrite and talc surfaces. The adsorption amount of CLS on the talc surface increased with the increase in the amount of CLS, and the adsorption amount of CLS on the talc surface was significantly higher than that on the chalcopyrite surface. After the addition of calcium ions, the adsorption capacity of CLS on chalcopyrite and talc increased, but the adsorption capacity on talc was significantly higher than that on chalcopyrite, which indicated that calcium ions were favorable for the adsorption of CLS on the surface of the talc.

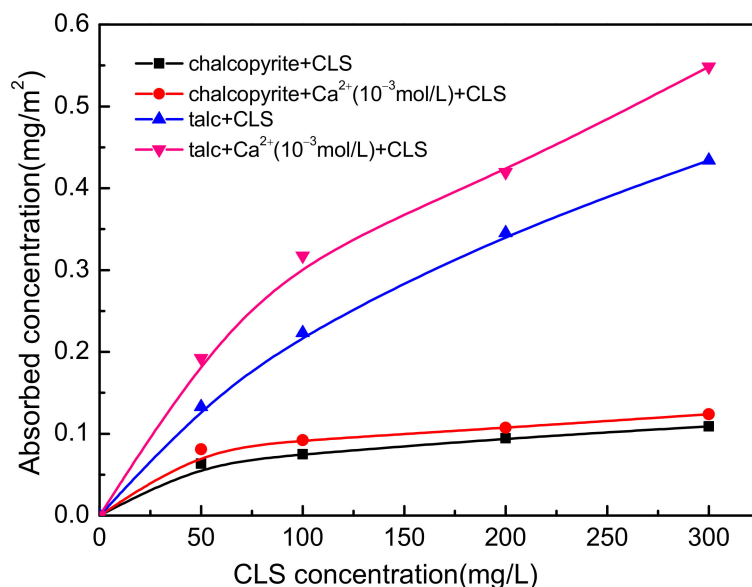


Figure 7. Adsorption behavior of CLS on chalcopyrite and talc with/without the presence of Ca^{2+} ions at pH 8.

3.3. Zeta Potential Measurements

Based on the results of the flotation tests, CLS and calcium ions were supposed to be an efficient combined depressant for chalcopyrite and talc flotation separation. Consequently, exploring the adsorption behavior of CLS/calcium ions on talc surface by zeta potential, FTIR, and AFM analyses is a meaningful objective. Figure 8 shows the zeta potentials of talc in the absence and presence of CLS. As can be seen from Figure 8, the isoelectric point pH of talc was about 2.1, and the surface of talc was negatively charged in a wide

range of pH values. When $\text{pH} < 3.7$, the zeta potential on the talc surface shifted negatively after CLS was added. When $\text{pH} > 3.7$, the zeta potential on the talc surface only shifted slightly. The above results indicated that the adsorption capacity of CLS on the talc surface in an acidic environment was stronger than that in an alkaline environment. This can be due to the fact that talc had a positive or small negative charge in the acidic environment, resulting in attraction forces or small repulsive forces between CLS and the talc in aqueous solution, which resulted in hydrogen bond formation and adsorption. However, talc had a more negative charge under alkaline conditions, so it did not readily adsorb negative CLS. Hence, the depression effect of CLS on talc in the alkaline environment was weaker than that in the acidic environment. Figure 9 exhibits the content of calcium ions at different pHs. After the addition of calcium ions, a positive shift in the zeta potential on the talc surface became obvious at $\text{pH} > 3.7$, which indicated that the presence of Ca^{2+} and $\text{Ca}(\text{OH})^+$ might promote the adsorption of CLS on talc and strengthen the depression effect of CLS. Ca^{2+} and $\text{Ca}(\text{OH})^+$ adsorbed on the talc, neutralized the negative charge on the surface of the talc, and generated the binding site with CLS, forming the $[\text{talc}-\text{Ca}^{2+}/\text{Ca}(\text{OH})^+-\text{CLS}]$ system.

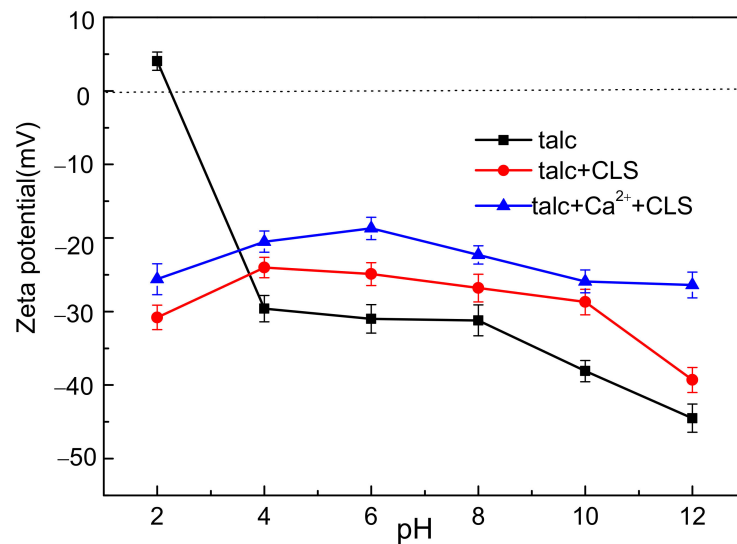


Figure 8. Effect of CLS on zeta potential values of talc with/without the presence of Ca^{2+} ions ($c(\text{CLS}) = 200 \text{ mg/L}$).

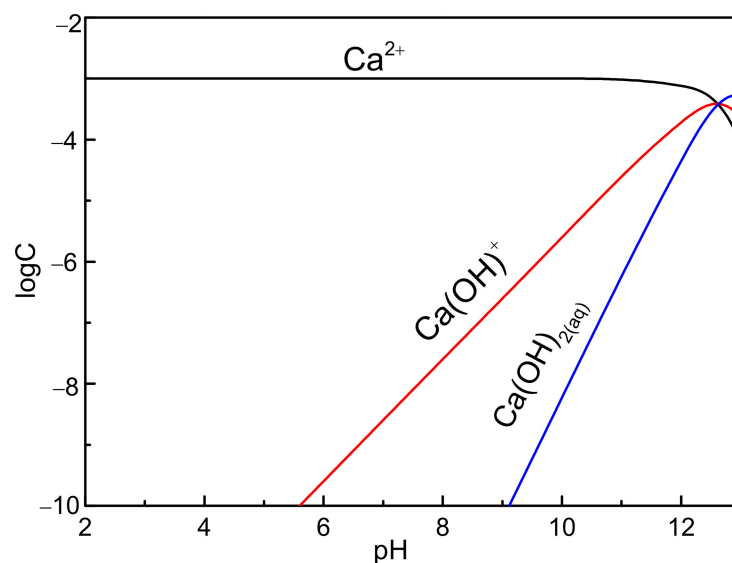


Figure 9. Calcium ion solution composition at different pH values.

3.4. FTIR Measurements

Figure 10 shows the results of the FTIR spectrum of CLS, and the peaks at 3387 cm^{-1} , 1648 cm^{-1} , 1042 cm^{-1} , and 617 cm^{-1} could be assigned to the stretching vibration peak of $-\text{OH}$, the stretching vibration peak of the benzene ring, the symmetric stretching peak of SO_3 sulfonate, and the asymmetric angular absorption peak of SO_4^{2-} sulfate, respectively [27,28]. An FTIR spectrum test was conducted on CLS samples after interaction with the talc, and the results are shown in Figure 11. Figure 11 describes the FTIR spectra before and after CLS treatment of talc in the presence and absence of calcium ions. For talc, the tensile vibration and bending vibration of Si-O appeared at 1018 cm^{-1} and 462 cm^{-1} , and the expansion peak and CO_2 absorption peak of crystal water appeared at 3677 cm^{-1} and 670 cm^{-1} . The addition of CLS resulted in two new peaks for talc, located at 3368 cm^{-1} and 1653 cm^{-1} and generated by $-\text{OH}$ and benzene ring stretching vibrations, respectively, indicating that CLS was adsorbed onto the talc surface. Two new peaks were observed on the talc after the addition of calcium ions, which were seen at 3400 cm^{-1} and 1634 cm^{-1} and were generated by the $-\text{OH}$ and benzene ring stretching vibration of CLS-2, respectively.

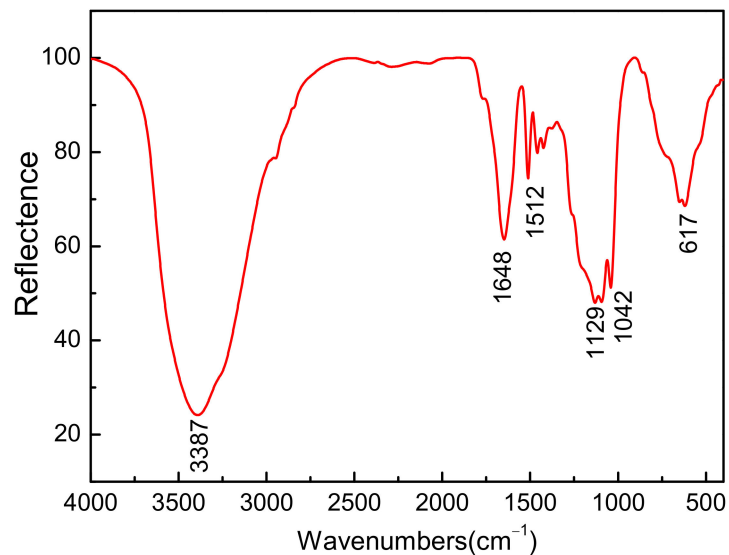


Figure 10. FTIR spectrum of CLS.

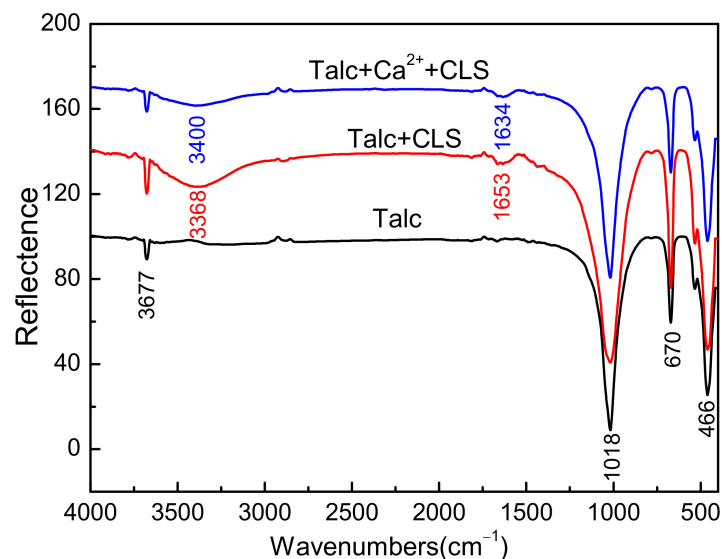


Figure 11. FTIR spectrum of talc conditioned with CLS with/without the presence of Ca^{2+} ions.

3.5. AFM Imaging Results

In order to study the effect of calcium ions on the adsorption behavior of CLS on the talc surface, the morphology of the CLS (200 mg/L, pH = 8) adsorption layer was studied by an AFM imaging method. Figure 12 shows the height and peak force error of exposed talc in the absence of CLS. Figures 13 and 14 show the AFM images (height, peak force error, and 3D images) of CLS adsorbed on the talc surface with or without additional calcium ions. The AFM height map and 3D image reflect the adsorption morphology of the agent on the talc surface, while the peak force error image provides details of the difference in the deformation ability of the material surface, which is directly controlled by using the peak force as the feedback parameter.

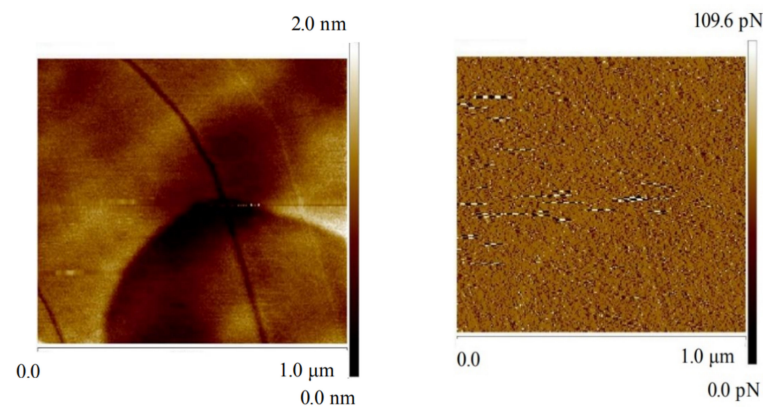


Figure 12. Height and Peak Force Error image of bare talc ($c(\text{CLS}) = 0 \text{ mg/L}$, $\text{pH} = 8$).

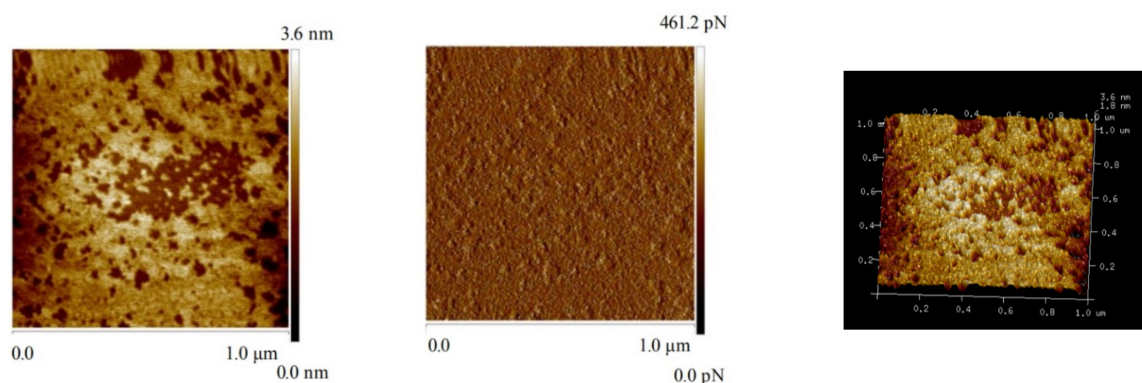


Figure 13. Height, Peak Force Error, and 3D image of talc treated with CLS ($c(\text{CLS}) = 200 \text{ mg/L}$, $\text{pH} = 8$).

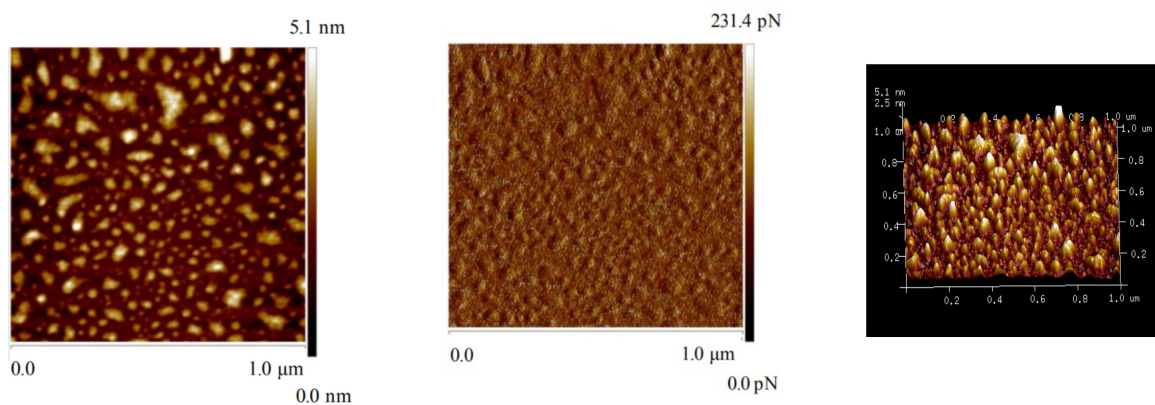


Figure 14. Height, Peak Force Error, and 3D image of talc treated with CLS and Ca^{2+} ($c(\text{CLS}) = 200 \text{ mg/L}$, $c(\text{Ca}^{2+}) = 1 \times 10^{-3} \text{ mol/L}$, $\text{pH} = 8$).

As shown in Figure 13, in the absence of Ca^{2+} ions, CLS still had a certain adsorption capacity on the talc surface. The AFM image of CLS on the talc showed that CLS was adsorbed on the talc surface in a flocculating network, but the low content of calcium ions was not enough to overcome the electrostatic repulsion between the talc surface and CLS, and the hydrophobic groups of CLS were not well dispersed on the talc surface. Figure 14 shows the AFM diagram of CLS after the addition of the Ca^{2+} (1×10^{-3} mol/L) solution. As can be seen from Figure 14, CLS was independently and densely adsorbed on the talc surface in a dispersive form, and the additional Ca^{2+} caused CLS to change from a flexible collapsed state into a highly dense shape. Combined with the previous zeta potential detection analyses, the [Talc- Ca^{2+} /Ca(OH) $^{+}$ -CLS] system was beneficial to overcome the electrostatic repulsion between the talc surface and CLS, so that the hydrophilic groups of CLS were arranged independently and orderly on the talc surface, which greatly increased the hydrophilicity of the talc surface.

The sample roughness root mean square (RMS), peak-to-valley distance (PTV), apparent layer thickness (Δ PTV), and surface coverage are shown in Table 3. When CLS interacted with the talc, the Δ PTV without added calcium ions was 0.831 nm, and the Δ PTV with added calcium ions was 0.915 nm, which indicated that CLS was adsorbed on the surface of talc in multiple layers. After calcium ions were added, the adsorption layer of CLS on the surface of talc became thicker. The coverage rate of CLS on the surface of the talc without added Ca^{2+} was 76.75%, and the coverage rate of CLS on the surface of the talc with added Ca^{2+} was 91.46%. Compared with no added Ca^{2+} , the coverage rate of CLS adsorbed on the talc was significantly improved, which indicated that the addition of calcium ions was beneficial to the adsorption of depressant CLS on the surface of the talc.

Table 3. Morphological details (RMS, PTV, Δ PTV, and coverage) for CLS adsorbed on talc ($c(\text{CLS}) = 200$ mg/L, $c(\text{Ca}^{2+}) = 1 \times 10^{-3}$ mol/L, pH = 8).

Samples	RMS (nm) \pm 0.005	PTV (nm) \pm 0.005	Δ PTV (nm) \pm 0.005	Coverage (%)
Bare talc	0.275	0.176	-	-
Talc + CLS	1.17	1.007	0.831	76.75
Talc + Ca^{2+} + CLS	1.27	1.091	0.915	91.46

4. Conclusions

Several conclusions can be drawn from this study. Firstly, CLS had a strong depression effect on the talc, while calcium ions could enhance the depression effect of CLS on the talc though that the depression effect on chalcopyrite was weak. The flotation separation of chalcopyrite and talc can be achieved in a pH range of 6–12 by using the combined depressant of CLS and calcium ions. CLS mainly depressed the flotation of the talc by adsorbing on the talc surface. Ca^{2+} and Ca(OH) $^{+}$ could adsorb on the talc surface after the addition of calcium ions, which would neutralize the negative charge of the talc surface, create sites for binding with CLS, and subsequently form the [talc- Ca^{2+} /Ca(OH) $^{+}$ -CLS] system. Furthermore, results of AFM imaging showed that, in the absence of Ca^{2+} ions, CLS formed a flocculant network to adsorb on the talc surface. However, a dispersed and independent dense adsorption on the talc surface occurred when Ca^{2+} (1×10^{-3} mol/L) solution was added. The addition of Ca^{2+} transformed the CLS adsorption layer from a flexible collapsed state to a highly dense shape, which thickened the adsorption layer on the talc surface and significantly improved the coverage.

Author Contributions: Conceptualization, methodology, formal analysis, investigation, writing—original draft preparation and writing—review and editing, Q.M. and H.Z.; Q.M. and H.Z. contributed equally to this work; supervision and project administration, L.O. All authors have read and agreed to the published version of the manuscript.

Funding: This work was financially supported by the National Natural Science Foundation of China (No. 51674291), and the Fundamental Research Funds for the Central Universities of Central South University (No. 2020zzts738).

Conflicts of Interest: The authors declare no conflict of interest.

References

1. Seck, G.S.; Hache, E.; Bonnet, C.; Simoën, M.; Carcanague, S. Copper at the crossroads: Assessment of the interactions between low-carbon energy transition and supply limitations. *Resour. Conserv. Recycl.* **2020**, *163*, 105072. [[CrossRef](#)] [[PubMed](#)]
2. Liu, D.; Zhang, G.; Chen, Y.; Huang, G.; Gao, Y. Investigations on the utilization of konjac glucomannan in the flotation separation of chalcopyrite from pyrite. *Min. Eng.* **2020**, *145*, 106089. [[CrossRef](#)]
3. Jin, S.; Shi, Q.; Li, Q.; Ou, L.; Ouyang, K. Effect of calcium ionic concentrations on the adsorption of carboxymethyl cellulose onto talc surface: Flotation, adsorption and AFM imaging study. *Powder Technol.* **2018**, *331*, 155–161. [[CrossRef](#)]
4. Khraisheh, M.; Holland, C.; Creany, C.; Harris, P.; Parolis, L. Effect of molecular weight and concentration on the adsorption of CMC onto talc at different ionic strengths. *Int. J. Min. Process.* **2005**, *75*, 197–206. [[CrossRef](#)]
5. Mierczynska-Vasilev, A.; Beattie, D.A. The effect of impurities and cleavage characteristics on talc hydrophobicity and polymer adsorption. *J. Min. Process.* **2013**, *118*, 34–42. [[CrossRef](#)]
6. Morris, G.E.; Fornasiero, D.; Ralston, J. Polymer depressants at the talc-water interface: Adsorption isotherm, microflotation and electrokinetic studies. *J. Min. Process.* **2002**, *67*, 211–227. [[CrossRef](#)]
7. Kursun, H.; Ulusoy, U. Influence of shape characteristics of talc mineral on the column flotation behavior. *Int. J. Min. Process.* **2005**, *78*, 262–268. [[CrossRef](#)]
8. Mierczynska-Vasilev, A.; Beattie, D.A. Adsorption of tailored carboxymethyl cellulose polymers on talc and chalcopyrite: Correlation between coverage, wettability, and flotation. *Min. Eng.* **2010**, *23*, 985–993. [[CrossRef](#)]
9. Jin, S.; Shi, Q.; Feng, Q.; Zhang, G.; Chang, Z. The role of calcium and carbonate ions in the separation of pyrite and talc. *Min. Eng.* **2018**, *119*, 205–211. [[CrossRef](#)]
10. Lotter, N.O.; Bradshaw, D.J.; Becker, M.; Parolis, L.A.S.; Kormos, L.J. A discussion of the occurrence and undesirable flotation behaviour of orthopyroxene and talc in the processing of mafic deposits. *Min. Eng.* **2008**, *21*, 905–912. [[CrossRef](#)]
11. Zhao, K.; Gu, G.; Wang, C.; Rao, X.; Wang, X.; Xiong, X. The effect of a new polysaccharide on the depression of talc and the flotation of a nickel-copper sulfide ore. *Min. Eng.* **2015**, *77*, 99–106. [[CrossRef](#)]
12. Ilhwan, P.; Seunggwon, H.; Sanghee, J.; Mayumi, I.; Naoki, H. Flotation Separation of Chalcopyrite and Molybdenite Assisted by Microencapsulation Using Ferrous and Phosphate Ions: Part I. Selective Coating Formation. *Metals* **2020**, *10*, 1667.
13. Johnston, H.E. Reverse Flotation of a Chalcopyrite Concentrate. Bachelor's Thesis, University of Queensland, St Lucia, Australia, 2005.
14. Ahmed, M.M.; Ibrahim, G.A.; Hassan, M. Improvement of Egyptian talc quality for industrial uses by flotation process and leaching. *Int. J. Min. Process.* **2007**, *83*, 132–145. [[CrossRef](#)]
15. Farrokhpay, S.; Ndlovu, B.; Bradshaw, D. Behavior of talc and mica in copper ore flotation. *Appl. Clay Sci.* **2018**, *160*, 270–275. [[CrossRef](#)]
16. Parolis, L.A.; van der Merwe, R.; Groenmeyer, G.V.; Harris, P.J. The influence of metal cations on the behaviour of carboxymethyl celluloses as talc depressants. *Colloids Surf. A Phys. Eng. Asp.* **2007**, *317*, 109–115. [[CrossRef](#)]
17. Feng, B.; Zhang, W.; Guo, Y.; Peng, J.; Ning, X.; Wang, H. Synergistic effect of acidified water glass and locust bean gum in the flotation of a refractory copper sulfide ore. *J. Clean. Prod.* **2018**, *202*, 1077–1084. [[CrossRef](#)]
18. Liu, C.; Feng, Q.; Shi, Q. Utilization of N-carboxymethyl Chitosan as a Selective Depressant for Talc In Flotation of Chalcopyrite. *Min. Min.* **2019**, *55*, 108–115.
19. Pan, G.; Shi, Q.; Zhang, G. Selective depression of talc in chalcopyrite flotation by xanthan gum: Flotation response and adsorption mechanism. *Colloids Surf. A Phys. Eng. Asp.* **2020**, *600*, 124902. [[CrossRef](#)]
20. Liu, C.; Ai, G.; Song, S. The effect of amino trimethylene phosphonic acid on the flotation separation of pentlandite from lizardite. *Powder Technol.* **2018**, *336*, 527–532. [[CrossRef](#)]
21. Ma, X.; Pawlik, M. The effect of lignosulfonates on the floatability of talc. *Int. J. Min. Process.* **2007**, *83*, 1–2. [[CrossRef](#)]
22. Lim, Z.Q.; Aziz, N.A.A.; Idris, A.K.; Akhir, N.A.M. Green Lignosulphonate as co-surfactant for wettability alteration. *Pet. Res.* **2020**, *5*, 154–163. [[CrossRef](#)]
23. Liu, R.; Sun, W.; Hu, Y.; Wang, D. Effect of organic depressant lignosulfonate calcium on separation of chalcopyrite from pyrite. *J. Cent. South Univ. Technol.* **2012**, *16*, 753–757. [[CrossRef](#)]
24. Liu, C.; Zhu, G.; Song, S.; Li, H. Flotation separation of smithsonite from quartz using calcium lignosulphonate as a depressant and sodium oleate as a collector. *Miner. Eng.* **2019**, *131*, 385–391. [[CrossRef](#)]
25. Zhou, H.; Zhang, Z.; Ou, L.; Mai, Q. Flotation separation of chalcopyrite from talc using a new depressant carrageenan. *Colloids Surf. A Physicochem. Eng. Asp.* **2020**, *603*, 125274. [[CrossRef](#)]
26. Paredes, Á.; Acuña, S.M.; Toledo, P.G. AFM Study of Pyrite Oxidation and Xanthate Adsorption in the Presence of Seawater Salts. *Metals* **2019**, *9*, 1177. [[CrossRef](#)]

-
27. Le Guern, C.; Conil, P.; Houot, R. Role of calcium ions in the mechanism of action of a lignosulphonate used to modify the wettability of plastics for their separation by flotation. *Miner. Eng.* **2000**, *13*, 53–63. [[CrossRef](#)]
 28. Wang, L.; Zhou, W.; Song, S.; Gao, H.; Niu, F.; Zhang, J.; Ai, G. Selective separation of hematite from quartz with sodium oleate collector and calcium lignosulphonate depressant. *J. Mol. Liq.* **2020**, *322*, 114502. [[CrossRef](#)]